Scientia Iranica A (2023) 30(3), 891–901

Sharif University of Technology
Scientia Iranica
Transactions A: Civil Engineering
http://scientiairanica.sharif.edu

Semi-supported steel plate shear wall with oblique sides

V. Broujerdian[a,*], R. Pahnabi[a], and A. Ghamari[b]

a. *School of Civil Engineering, Iran University of Science and Technology, Tehran, Iran.*
b. *Department of Civil Engineering, Darreh Shahr Branch, Islamic Azad University, Darreh Shahr, Iran.*

Received 22 July 2021; received in revised form 31 December 2021; accepted 25 April 2022

KEYWORDS
Steel plate shear wall;
Semi-supported;
Finite element analysis;
ABAQUS;
Analytical method.

Abstract. This paper presents a new configuration of semi-supported steel plate shear wall to increase its efficiency. For this purpose, the infill steel plate is proposed to be trapezoidal instead of rectangular. In order to find the most efficient inclination angle of lateral sides, a numerical parametric study was conducted. Five different values of inclination angle including 60°, 75°, 90°, 105°, and 120° were considered. Furthermore, two thicknesses of 1.75 and 2.00 mm were considered for steel plate. The area of steel plate was the same for all the models. The models were analyzed using finite element software ABAQUS. Both geometric and material nonlinearities were considered. In order to validate the finite element modeling, the available experimental results were used. According to the results of comparing the wall with the rectangular plate, the inclination angle of 60° increased the ultimate lateral strength and stiffness of the 1.75 mm-thick wall by 46% and 66%, respectively. Furthermore, a simple approximate model was presented to calculate the load-deformation response of the proposed wall using SAP 2000 program. Despite the simplicity of the method, the results were in good agreement with the results of ABAQUS.

1. Introduction

Steel Plate Shear Wall (SPSW) is an efficient lateral load-resisting system that exhibited viable performance in past earthquakes as well as in laboratory studies [1,2]. The stiffness, strength, and high energy absorption of the system encouraged experts and engineers to use it in both new and retrofit projects. Now, many design codes of practice around the world have incorporated design provisions and guidelines for SPSW [3–7]. Early designs of SPSW system, about five decades ago, were based on its linear elastic behavior. Therefore, thick or stiffened steel plates were used at that time. However, engineers gradually began to realize that the nonlinear post-buckling reserve capacity of steel plate should be utilized to achieve an economic design [8–15]. Unstiffened SPSW relies on post-buckling behavior dominated by tension field action to withstand huge forces after buckling. Furthermore, this system is preferable to the stiffened type due to ease of construction.

Another step in understanding the behavior of the SPSW system was that connecting the steel plate to the main columns of the frame increased their design demands and consecutively increased the probability of their premature failure [16,17]. By forming a diagonal tension field in the steel plate, very large stresses are introduced to the surrounding columns demanding an uneconomical section design to avoid buckling. To improve the behavior of the system, researchers suggested using an innovative technique

*. *Corresponding author. Tel.: +98 21 73227158; Fax: +98 21 77240399*
E-mail addresses: broujerdian@iust.ac.ir (V. Broujerdian); ramin_pahnabi@alumni.iust.ac.ir (R. Pahnabi); aghamari@alumni.iust.ac.ir (A. Ghamari)

doi: 10.24200/sci.2022.58749.5882

in which instead of attaching the steel plate to the main columns, it attaches to the secondary columns [8,9,18–22]. Therefore, the large stresses due to the post-buckling diagonal tension field transfer to the secondary columns and the capacity of the main columns remains free to act as a frame member. This system is called semi-supported steel plate sheer wall. In addition to its structural advantages over the conventional SPSW, the semi-supported SPSW system enjoys architectural advantages as it reduces the size of columns and provides the possibility to locate openings.

Despite the advances made so far in the use of steel shear walls, one of the shortcomings in this regard is the imperfect diagonal tension field formed in the steel plate. This problem prevents use of the full capacity of steel plate. In fact, the portions of the steel plate that are farther away from the main tensile diameter have a less share of load-bearing capacity. Therefore, it is not possible to form a complete plastic tensile field and some parts remain elastic. This is the reason why the entire material capacity is not to be used and it reduces the system efficiency. Research on improving the efficiency of the SPSW system is still ongoing and these efforts are far from being settled [20,23–30].

In spite of the good performance of the SPSW in recent earthquakes and experimental studies, the need for huge columns to surround the infill plate is a major shortcoming of the system. This shortcoming can be resolved by using a semi-supported SPSW. The semi-supported SPSW has secondary columns that prevent the transfer of stress from the infill plate to the main columns. In spite of extensive experimental and numerical investigations into SPSWs, there are many ambiguities regarding the behavior of the semi-supported SPSW. This study aims to enhance and improve the performance of the semi-supported SPSW by changing the geometry of the steel plate. Both the shape and thickness of the steel plate are modified to increase the efficiency of the system, but the volume of steels is equal for all models. To this end, first, Oblique Semi-supported Steel Plate Shear Wall (OS-SPSW) is introduced. Then, a numerical parametric study to optimize the geometry of the proposed system is performed using finite element method. The numerical simulation and analyses are performed using the general-purpose finite-element software package ABAQUS. In order to validate the numerical results, the available experimental data are used. Finally, because of the complexity of the modeling process of such a system in ABAQUS, a simple approximate method is presented based on finite-element software SAP2000, as well. The proposed approximate method replaces the OS-SPSW system with an equivalent bracing system. Then, SAP2000 is used to calculate its load-deformation curve. The process of modeling in SAP2000 is much easier for engineers than ABAQUS. The proposed simple approach is capable of calculating the load-displacement curve considering linear and nonlinear behaviors. To assess the robustness of the proposed simple method, the results are corroborated with the exact finite-element simulations of ABAQUS.

2. Method of study

2.1. Introducing the OS-SSPSW

The core idea of using a thin SPSW system is to utilize the diagonal tension field. The strength of this system is mainly due to the post-buckling resistance of thin plates, or in fact, the resistance due to the diagonal tension field created after the buckling of the steel plate. When SPSW is subjected to lateral forces, the steel web plate sustains compressive and tensile stresses in diagonal directions before buckling. Naturally, the steel plate cannot withstand the compressive stress. However, the plate can sustain tensile stresses up to its yield point. Therefore, if the applied forces are increased so that the compressive stress in the web exceeds the critical stress, the plate will buckle and become distorted, but it still can withstand significant forces. The columns attached to the SPSW must be designed such that they would not yield or buckle before the plate is yielded due to the diagonal tensile field. To reduce the design demand of the main columns, steel plate is not connected to the main columns in a semi-supported SPSW. As shown in Figure 1, the steel plate is built separately with its border elements (secondary columns).

In the semi-supported SPSW, the secondary columns only carry compressive stresses induced by the tension field of the plate and the gravity loads of the building are carried separately by the main columns. Furthermore, with the use of a semi-supported shear wall system, it is possible to insert an opening in the distance between the main columns of the structure. Therefore, the architectural considerations may be largely implemented.

Besides the advantages of a semi-supported steel shear wall, one main deficiency is that some parts of the steel plate remain elastic. It means that the

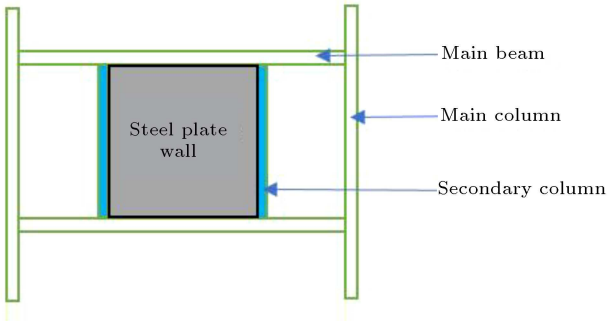

Figure 1. Ordinary semi-supported SPSW.

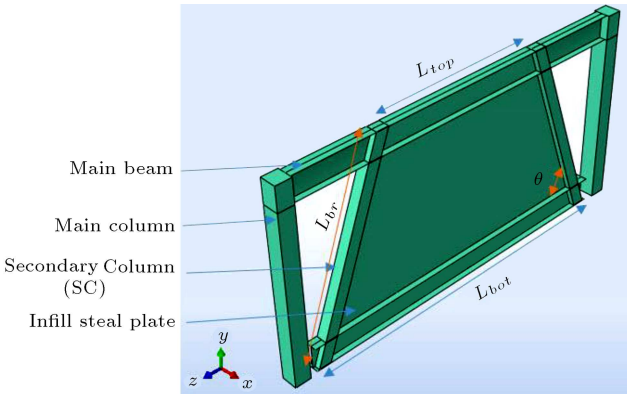

Figure 2. Oblique semi-supported steel plate shear wall.

entire capacity of the steel plate is not used. To increase the efficiency of the system, the infill plate and the secondary columns surrounding the infill plate are suggested to be skewed, as shown in Figure 2. The main idea is to locate the material closer to the direction of principal tensile stresses. The behavior of the proposed system is investigated numerically and analytically in this study.

2.2. Numerical modeling

2.2.1. Specifications of the numerical models

To evaluate the basic behavior of the proposed OS-SPSW system, a single-story single-bay frame fixed at the base is considered here. The lateral load is applied to the beam-column connection and is increased monotonically from zero. The ultimate displacement limit is considered to occur at a drift ratio of 2.5% per ASCE 7 [31]. All steel components are assumed to be made from ST37 steel with a yield stress of 240 MPa, ultimate stress of 370 MPa, Young's modulus of 200 GPa, and Poisson's ratio of 0.3. The constitutive behavior of steel is assumed to be elastic-perfectly plastic. To define the 3D plasticity of steel, von Mises yield criterion and the associated flow rule are used [18].

Specifications of the simulated models are summarized in Table 1. As seen in this table, different inclination angles, θ, and two different plate thickness, t_w, were included in the selected set of models. Inclination angles range from 60° to 90°. It must be noted that the angle less than 60° is impossible due to executive problems. As the height and the total area of the steel plates are considered to be constant for all the models, the parameters of L_{bot} and L_{top} may be calculated for each value of θ. As depicted in Table 1, the aspect ratios, L_{bot}/L_{top}, range from 0.4 to 2.5. The cross-section of beams, main columns, and the secondary columns are IPE240, 2*IPE160, and 2*UNP120, respectively. All the connections are assumed to be rigid. Different angles have been considered for the steel sheet to form a full diagonal tension field.

2.2.2. Finite element details

The numerical simulation and analyses are performed using finite element software package ABAQUS. To provide more realistic simulations, all the members of the system including top beam, anchor beam, main columns, secondary columns, and infill plate are modeled using shell elements. There is a variety of shell elements in ABAQUS, each of which has a different behavior. This study employs a four-node quadrilateral doubly curved S4R element. It is a general-purpose shell element with reduced integration considering finite membrane strain and large rotations. This element takes into account the effects of transverse shear deformation and thickness change. The behavior of this element for thin plates is consistent with the classical plate theory. Both material and geometric nonlinearities are considered. To consider the imperfection effect, a buckling analysis was performed first. Then, the first buckling mode with a coefficient of 1/1000 was introduced to the software. Therefore, the structure included imperfection to consider the geometric nonlinear effects. The analyses were done using general static and modified risk methods capable of detecting the full equilibrium path of the structure. To

Table 1. Properties of the specimens used for optimization of the geometry.

Model no.	t_w (mm)	τ (degree)	$L_{bot}\,(m)$	$L_{top}\,(m)$	$\frac{L_{bot}}{L_{top}}$
S-60-1.75	1.75	60	4.3	1.7	2.50
S-60-2.00	2.00	60			
S-75-1.75	1.75	75	3.6	2.4	1.50
S-75-2.00	2.00	75			
S-90-1.75	1.75	90	3.0	3.0	1.00
S-90-2.00	2.00	90			
S-105-1.75	1.75	105	2.4	3.6	0.7
S-105-2.00	2.00	105			
S-120-1.75	1.75	120	1.7	4.3	0.40
S-120-2.00	2.00	120			

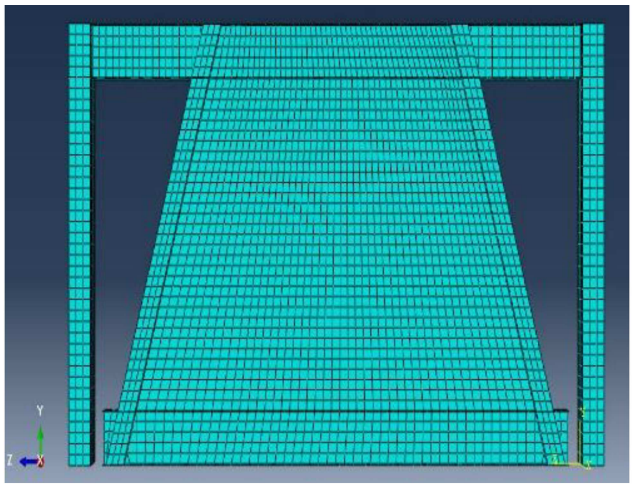

Figure 3. Semi-supported steel plate shear wall meshing.

simulate the post-buckling behavior of the infill plate, a multiple of the first Eigen-mode system obtained from the elastic buckling analysis is adopted as initial imperfection [18,32].

All the components are meshed such that their nodes adhere to adjoining elements and make a complete connection. All supports are of fixed supports. To simulate the constraints imposed by slabs of the story floors, the out-of-plane displacements of top beam webs are restrained, as well. The finite element model of an oblique semi-supported wall generated by ABAQUS is shown in Figure 3.

2.2.3. Verification of the numerical modeling process

In order to verify the adequacy of finite element modeling to calculate the load-displacement response of the semi-supported SPSW, an experimental test conducted on an ordinary semi-supported SPSW [33] is considered as benchmark. The test setup is shown in Figure 4. As seen in this figure, a monotonic load was applied to the ends of the top beam. The cross-section of beams, main columns, and secondary columns were

Figure 4. Setup of experimental test [19].

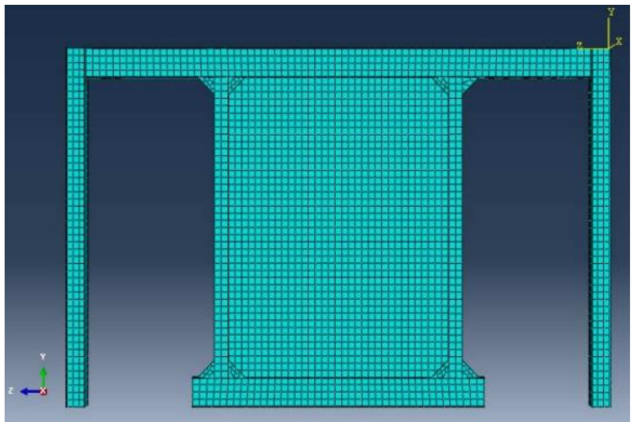

Figure 5. Finite element model of experimental test.

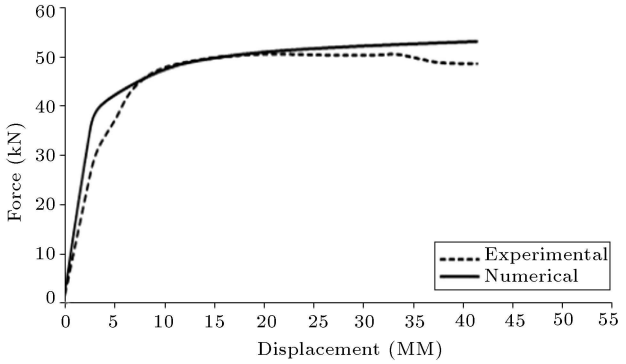

Figure 6. Comparison of numerical modeling results with the experimental results.

IPE240, 2*IPE160, and 2UNP160, respectively. The thickness of the steel plate was 2 mm. By considering the material properties, the geometric specifications, and the loading as well as boundary conditions reported in the benchmark study, a finite element simulation is conducted. The corresponding meshed model generated by ABAQUS is shown in Figure 5 [34,35].

According to the test report, the ultimate capacity of the system is equal to 74 ton which is very close to 72 ton as the ultimate capacity predicted by the FEM simulation, with a maximum difference of 2.7%. Figure 6 compares the load-drift diagram derived from the current finite element push-over analysis to the envelope of the test specimen hysteresis curves. As seen in this figure, there is good agreement between the numerical model and that of the experimental test.

2.3. Proposed approximate method

Past studies showed that the middle diagonal strip of the steel plate panel had the greatest effect on the equivalent stiffness of the system [33]. Therefore, the stiffness of this strip can be used as a measure to determine the equivalent system. In order to calculate the cross-sectional area of the bracing equivalent to the steel shear wall, their elastic stiffness is considered to be equal. The proposed equivalent model shown in Figure 7 entails the following assumptions:

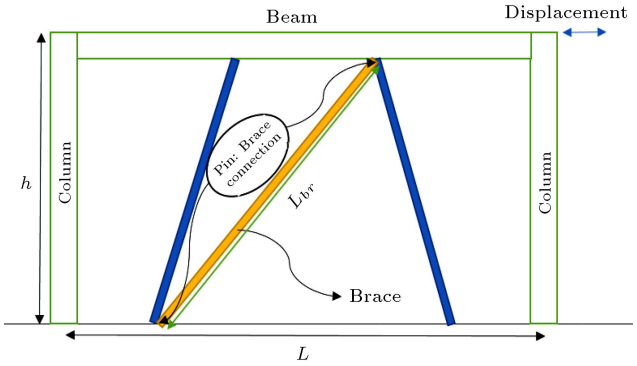

Figure 7. Bracing system equivalent to oblique semi-supported SPSW.

- The constitutive behavior of steel is elastic-perfectly plastic;
- The tensile field in the oblique plate formed after buckling is uniform throughout the plate;
- The effects of bending stresses on the shear stresses of the plate are ignored;
- Shear displacement of the steel plate during bending can be calculated from multiplying the shear strain by the panel height.

Prior to the critical shear stress required for buckling of the steel plate, equal tensile and compressive stresses are developed in the plate. The critical shear stress is calculated from the classical theory of stability according to the following equation:

$$\tau_{cr} = \frac{K_v \pi^2 E}{12(1-\upsilon^2)}(t/b)^2, \tag{1}$$

where τ_{cr} is the critical shear stress, υ Poisson's ratio, E the modulus of elasticity, t plate thickness, b the shear panel width, and K_v the plate buckling coefficient, which is calculated based on the aspect ratio given as follows [33]:

$$K_v = 5.34 + \frac{4}{(d/b)^2} \qquad \frac{d}{b} \leq 1, \tag{2}$$

$$K_v = 4 + \frac{5.34}{(d/b)^2} \qquad \frac{d}{b} \geq 1. \tag{3}$$

Theoretically, if the steel plate is thick enough so that the critical shear stress exceeds the shear yield stress, the steel plate could reach the yield point. Considering von Mises yield surface, shear yield stress, τ_y, is related to tensile yield stress, F_y, as:

$$\tau_y = \frac{F_y}{\sqrt{3}}. \tag{4}$$

If the steel plate is thin and buckles before yielding, the plate will not be able to withstand more compressive stresses. However, tensile stresses may still increase until the steel plate yields (Figure 8). Thus, a new bearing mechanism is created by the gradual formation of the tensile field after buckling of the plate and its spreading throughout the surface.

Principal direction of stresses in the steel plate is a function of loading and geometry. However, the approximate assumption of 45°enjoys enough accuracy. If the tensile field angle of 45° is assumed, the in-plane stresses equivalent to the yielding of the steel plate without considering the buckling critical stresses are equal to:

$$\sigma_{xx} = \sigma_{ty} \sin^2\theta, \tag{5}$$

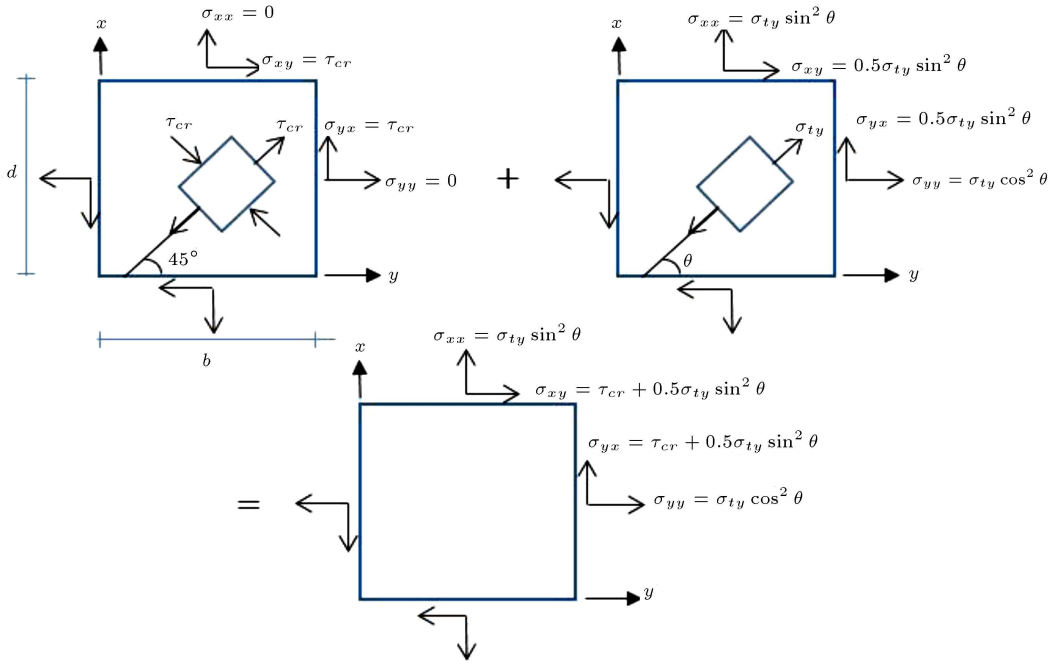

Figure 8. Stress status of steel plate before and after plate buckling.

$$\sigma_{yy} = \sigma_{ty}\cos^2\theta, \tag{6}$$

$$\tau_{xy} = \tau_{cr} + 0.5F_{ty}\sin 2\theta. \tag{7}$$

Referring to the state of stresses in Figure 8 and considering von Misses yield criterion, the stresses of tensile field corresponding to the yielding of the plate can be calculated as follows:

$$(\sigma_{xx} - \sigma_{yy}) + {\sigma_{yy}}^2 + {\sigma_{xx}}^2 + 6{\tau_{xy}}^2 - 2{\sigma_0}^2 = 0. \tag{8}$$

By substituting Eqs. (5)–(7) into Eq. (8), the following equation is obtained so as to calculate the stress at which the plate yields:

$$3{\tau_{cr}}^2 + 3{\tau_{cr}}^2\sigma_{ty}\sin 2\theta + {\sigma_{ty}}^2 - \sigma_0 = 0. \tag{9}$$

In this case, the shear force in which plate yields will be equal to:

$$\left(\frac{1}{4}\sigma_{ty}\sin 2\theta\right) t_w b U_{wpb} = \frac{{\sigma_{ty}}^2}{2E} hb.$$

$$V_{uw} = bt\left(\tau_{cr} + \frac{1}{2}\sigma_{ty}\sin 2\theta\right). \tag{10}$$

Upon applying the principles of energy-based plastic analysis and equalizing two levels of displacement, the yield limit displacement is calculated as follows:

$$\left(\frac{1}{4}\sigma_{ty}\sin 2\theta\right) t_w b U_{wpb} = \frac{{\sigma_{ty}}^2}{2E} hb, \tag{11}$$

where h is the frame height and U_{wpb} is the yield limit displacement of the system. Moreover, the shear displacement of the plate, U_w, equals:

$$U_w = \left(\frac{\tau_{cr}}{G} + \frac{2\sigma_{ty}}{E\sin 2\theta}\right) d, \tag{12}$$

where G is the shear modulus of the plate. With the shear force obtained from Eq. (10) and the shear displacement from Eq. (12), the shear stiffness of the steel plate equals:

$$K_w = \frac{bt}{d}\frac{\tau_{cr} + 0.5\sigma_{ty}\sin 2\theta}{\frac{\tau_{cr}}{G} + \frac{2\sigma_{ty}}{E\sin 2\theta}}. \tag{13}$$

On the other hand, the axial stiffness of the diagonal element may be converted into shear stiffness using the bracing angle relative to the horizon and is equal to:

$$K_{br} = \frac{EA}{L_{Br}}\cos^2\theta, \tag{14}$$

where L_{Br} is the brace length, E the modulus of elasticity, and A the cross-sectional area of the brace. Further, by equalizing the shear deformation of the diagonal brace, Δ_{Brace}, and that of the steel plate, U_w,

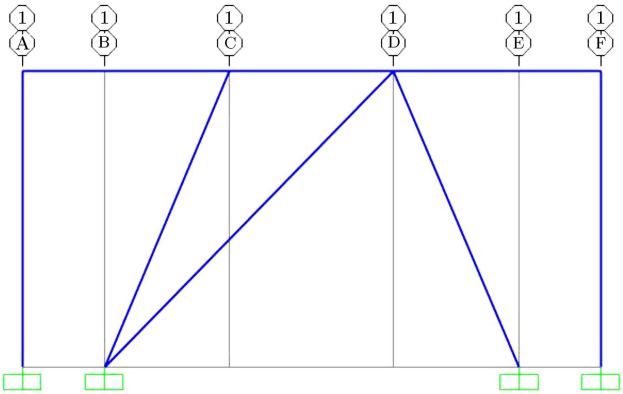

Figure 9. Equivalent single diagonal element generated by SAP 2000.

the cross-sectional area of the equivalent single brace, A_{Br}, may be calculated as follows:

$$A_{Br} = \frac{L_{Br}t_w b}{2.6h^2}. \tag{15}$$

Now, the equivalent bracing model may be simply simulated using finite element program SAP 2000 (Figure 9). Fixed supports at the base of the main and secondary columns are considered. The plastic joints of the columns and beam are considered at two ends of the elements. The plastic joint of equivalent diagonal element is defined at its middle point. In this research, auto plastic joint of SAP 2000 is used. The applied force is considered as one-way displacement.

3. Results and discussion

3.1. Pushover curves

The lateral load-displacement diagram contains valuable information based on which the overall behavior of the shear wall can be evaluated and the seismic parameters may be extracted. In order to estimate the values of seismic parameters, the actual load-displacement response curves are usually idealized, as illustrated in Figure 10. This idealization is based on the following assumptions and definitions:

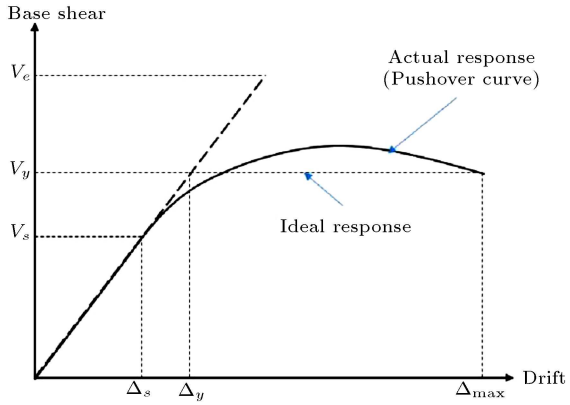

Figure 10. Idealization of the lateral load-displacement curve [36-38].

- The maximum displacement of the structure, Δ_{max}, will be considered based on the requirements of the local regulations. Here, the maximum displacement corresponds to 100 mm based on a drift ratio of 2.5%;
- The yield displacement, Δ_{max}, is measured based on the concept of equal plastic energy, such that the area under the idealized bilinear curve is the same as that under the actual pushover curve, as depicted in Figure 10;
- The Ductility factor is $\mu = \Delta_{max}/\Delta_y$.

Figures 11 and 12 present the lateral load-displacement curves of the numerical models with plate thicknesses of 1.75 mm and 2 mm, respectively. The pushover curves plotted in these figures reveal that the wall behavior clearly improves upon decreasing the inclination angle of steel plate. Meanwhile, obtuse angles decrease the efficiency of the system.

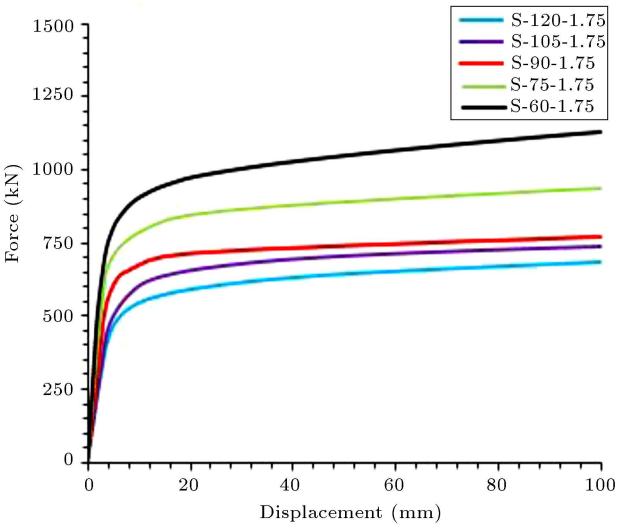

Figure 11. Lateral load-drift curves of numerical models with a plate thickness of 1.75 mm.

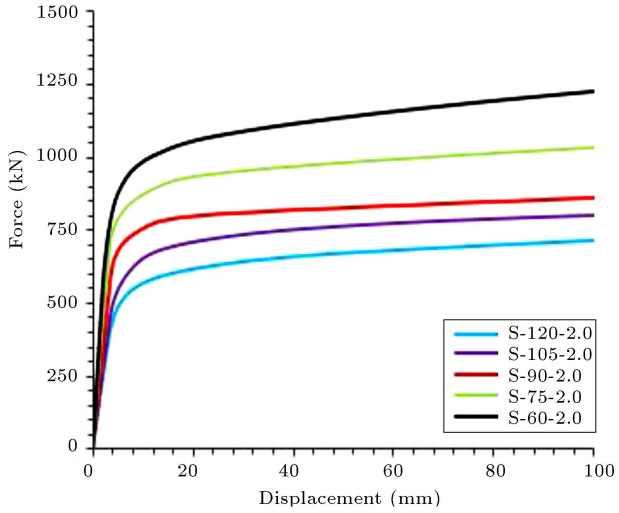

Figure 12. Lateral load-drift curves of numerical models with a plate thickness of 2 mm.

To shed light on the cause of the improvement of wall behavior with decreasing the inclination angle, von Mises stress contours are investigated in state of the maximum displacement. For this purpose, von Mises stress contours of models S-120-2.0, S-90-2.0, and S-60-2.0 are compared in Figure 13. These models have a similar plate thickness of 2.0 mm, but different inclination angles of 120°, 90°, and 60° respectively. As seen in Figure 13(a), in the model with an angle of 120°, plastic hinges are formed at several zones including link beams between the main columns and the secondary columns, two ends of the main columns, bottom and mid-height of secondary columns, and base of the infill plate. However, Figure 13(b) shows that in the model with an angle of 90°, plastic hinges are formed in the panel zones, at the bases of secondary columns, and in infill plate. Finally, Figure 13(c) shows that in the model with an angle of 60°, only the infill plate undergoes plastic deformation, whereas the main frame remains elastic. It means that the infill plate could behave as a ductile fuse against seismic loads.

3.2. Strength

The ultimate strength of a system is the maximum force that the system can withstand before failure. The less the strength of a system, the more the ductility demand. For the sake of comparison, the ultimate shear strengths of the numerical models with different thicknesses and inclination angles of plates are listed in Table 2. As seen in this table, the shear strength significantly decreases with increasing the steel plate angle while the plate thickness is constant. The third column of this table represents the ratios of ultimate strength of models with the same inclination angle but having different thicknesses. Two thicknesses of 1.75 and 2.00 mm are evaluated in this study. As seen in Table 2, increase in the plate strength due to thickness changes is between 5% and 11%.

Table 2. Ultimate strength of numerical models.

Model	F_u(kN)	$\frac{F_u(2.00\ mm)}{F_u(1.75\ mm)}$	$\frac{F_u(\theta)}{F_u(90°)}$
S-60-1.75	1128	1.09	1.46
S-60-2.00	1226		1.43
S-75-1.75	939	1.10	1.22
S-75-2.00	1034		1.20
S-90-1.75	773	1.11	1.00
S-90-2.00	859		1.00
S-105-1.75	737	1.09	0.95
S-105-2.00	803		0.94
S-120-1.75	681	1.05	0.88
S-120-2.00	717		0.84

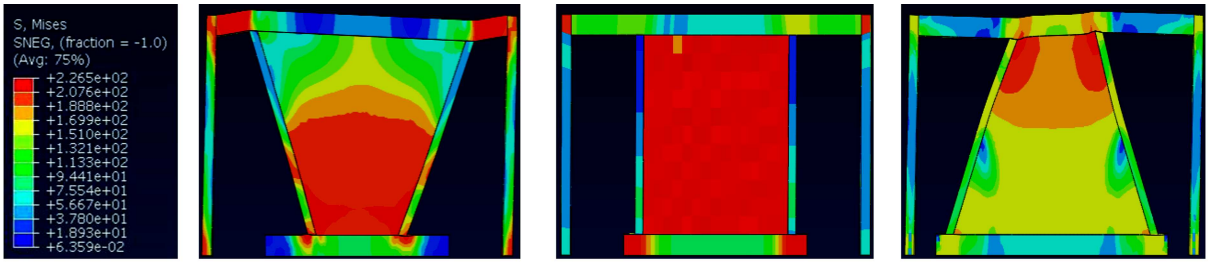

Figure 13. Von Mises stress contours of finite element models at maximum displacement: (a) S-120-2.0 model, (b) S-90-2.0 model, and (c) S-60-2.0 model.

The fourth column of Table 2 represents the ratio of ultimate strength of oblique models to one of the models with vertical plate ($\theta = 90°$) having the same thickness. As seen, increasing θ from 90° to 120° results in 12% and 16% rates of decrease in the ultimate strength for 1.75- and 2-mm-thickness models, respectively. However, decreasing θ from 90° to 60° leads to 46% and 43% increases in the ultimate strength of the models with 1.75 and 2 mm thickness, respectively. Generally, the effect of inclination angle is greater for the thinner steel plate.

3.3. Elastic and inelastic stiffness

The greater the lateral stiffness of a system is, the less displacement and drift it has during earthquake. Moreover, the lower the displacement is, the greater the safety and comfort of residents and users is. A structure whose stiffness is low may be destroyed by an earthquake and in this case, the effects of $P - \Delta$ are increased, thus not being suitable for a structure. Therefore, it is necessary to examine the stiffness.

The stiffness curves of the numerical models with 1.75 and 2 mm thicknesses are presented in Figures 14 and 15, respectively. As shown in these figures, the initial elastic stiffness significantly decreases with increasing the steel plate angle while the plate thickness remains constant. It can also be seen from Figures 14 and 15 that the inelastic stiffness of all the models with the same thickness converges to a constant value at a displacement of approximately 7 mm. It is noteworthy that at larger displacements, the stiffness reaches zero and never becomes negative. In fact, the system does not fail until the end of the loading process corresponding to the lateral displacement of 100 mm (drift ratio of 2.5%). Furthermore, based on the comparison of the curves of Figures 14 and 15, it appears that the elastic stiffness changes slightly as the thickness varies.

Table 3 summarizes the initial stiffness of the numerical models. As seen in this table, the increase in stiffness due to thickness changes is between 8% and 33%. Increasing θ from 90° to 120° results in 24% and 31% decrease in the stiffness of models with 1.75 and 2 mm thicknesses, respectively. However, decreasing

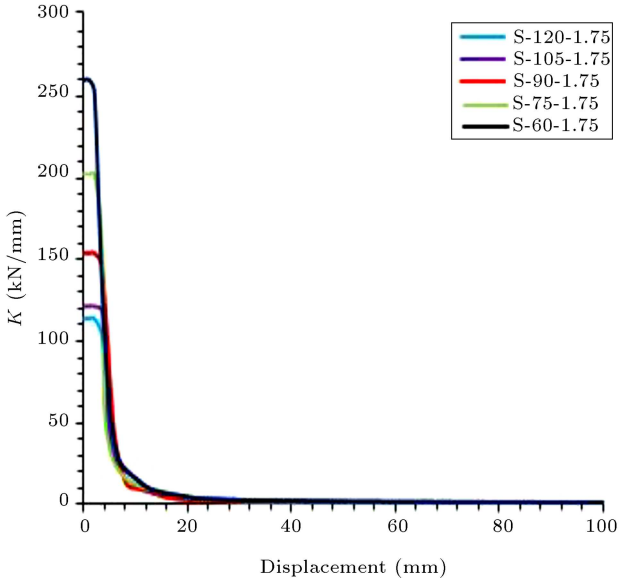

Figure 14. Stiffness versus displacement for the numerical models with a thickness of 1.75 mm.

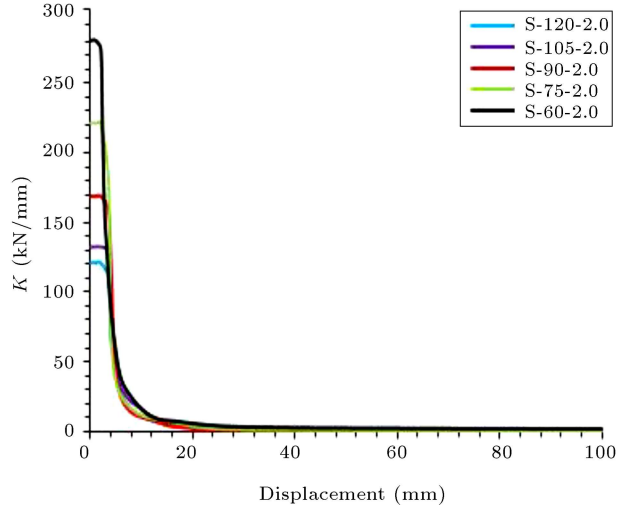

Figure 15. Stiffness versus displacement for the numerical models with a thickness of 2 mm.

θ from 90° to 60° leads to 66% and 44% increase in the initial stiffness of 1.75- and 2-mm-thickness models, respectively. Generally, the effect of inclination angle on stiffness is greater for the thinner steel plate.

Table 3. Initial stiffness of numerical models.

Model	K_0 (kN/mm)	$\frac{K_0(2.00\ mm)}{K_0(1.75\ mm)}$	$\frac{K_0(\theta)}{K_0(90°)}$
S-60-1.75	197.1	1.08	1.66
S-60-2.00	212.7		1.44
S-75-1.75	177.3	1.12	1.50
S-75-2.00	198.3		1.34
S-90-1.75	118.5	1.25	1.00
S-90-2.00	147.8		1.00
S-105-1.75	95.2	1.33	0.80
S-105-2.00	126.2		0.85
S-120-1.75	90.1	1.14	0.76
S-120-2.00	102.3		0.69

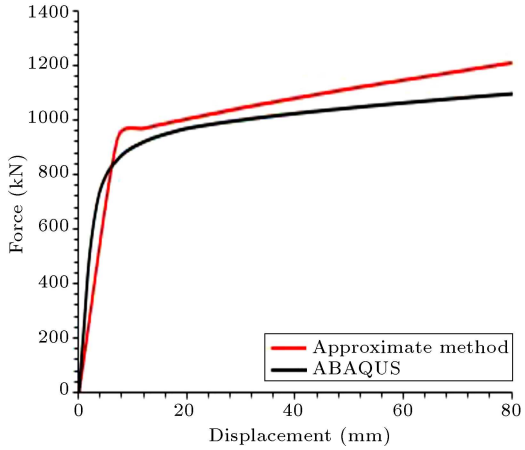

Figure 16. Comparing the pushover curves of S-60-1.75 obtained by the approximate method and ABAQUS.

3.4. Comparison of the proposed analytical and numerical methods

In order to verify the viability of the proposed approximate method, the results of ABAQUS for two models of S-60-1.75 and S-60-2.0 are compared with the results of SAP 2000 program. The pushover curves of the approximate method are derived from SAP 2000 and the results of the steel wall analysis in ABAQUS for S-60-1.75 and S-60-2.0 are compared in Figures 16 and 17, respectively. As seen in these figures, in spite of its simplicity, the approximate method exhibits a good correlation with ABAQUS results in terms of the ultimate strength and the overall behavior.

4. Conclusions

In this study, a new configuration of the semi-supported shear wall was presented in which the steel plate and secondary columns were inclined relative to the vertical state. By examining different inclination angles, it was observed that the oblique models having a sharp angle with the bottom horizon line performed better than the conventional vertical-side steel plates. Furthermore, a semi-analytical approximate model was proposed to

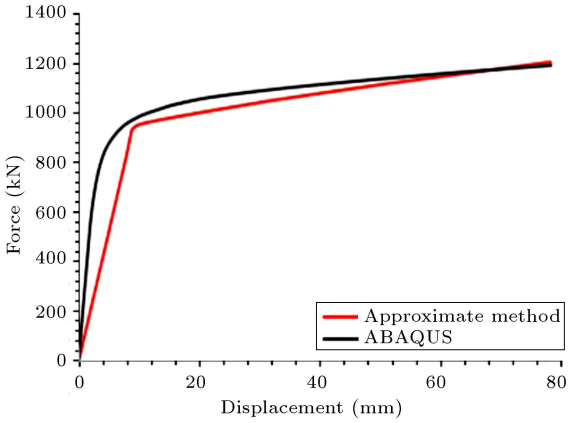

Figure 17. Comparing the pushover curves of S-60-2.0 obtained by the approximate method and ABAQUS.

calculate the pushover curve of the system by means of SAP 2000 engineering software. A summary of the results is as follows:

- If the steel wall angle is reduced compared to an upright position without changing the thickness and area of the steel plate, the strength, energy absorption, and stiffness of the frame increase;
- As the inclination angle of steel plate decreases, there will be more limited regions of the frame elements which undergo plastic deformation, and vice versa. In the case of the 60-degree-angle of steel plate, no plastic joint is formed in the main frame as well as the secondary columns up to 2.5% drift. It means that without forming a plastic joint in the frame, the steel wall experiences a nonlinear behavior which is a desired behavior against seismic loads;
- The thinner the steel plate of the shear wall, the greater the increased effect of inclination angle on the lateral strength and stiffness;
- Decreasing the angle from 90° to 60° leads to 46% and 43% increase in the ultimate strength of the models with 1.75 and 2 mm thicknesses, respectively;
- Decreasing the angle from 90° to 60° leads to 66% and 44% increases in the initial stiffness of 1.75- and 2-mm-thickness models, respectively. Generally, the effect of inclination angle on lateral strength and stiffness is greater for the thinner steel plate;
- In a percentage-wise comparison, the effect of inclination angle on lateral stiffness is greater than the one on lateral strength;
- An approximate method for nonlinear analysis of steel shear wall was presented, whereby the steel plate was replaced by an equivalent single truss element followed by a nonlinear analysis using SAP 2000 program. Since the steel plate is replaced

with a truss diagonal element, the analysis time is significantly reduced. Comparison of the results with the ones obtained by ABAQUS shows that the proposed approximate method has acceptable accuracy to predict strength, stiffness, and load-deformation curve of the system.

References

1. Berman, J.W., Lowes, L.N., Okazaki, T., et al. "Research needs and future directions for steel plate shear walls", *Structures Congress* 2008: Crossing Borders, pp. 1–10 (2008).
2. Astaneh-Asl, A. "Seismic Behavior and Design of Steel Shear Walls", *Structural Steel Educational Council Moraga*, CA, USA (2001).
3. AISC, "Specification for structural steel buildings", *American Institute of Steel Construction*, Chicago (2016a).
4. AISC, "Seismic provisions for structural steel buildings", *American Institute of Steel Construction*, Chicago (2016b).
5. Canadian Standards Association, *Limit States Design of Steel Structures*-CAN/CSA-S16; Rexdale, Ontario (2014).
6. Ali, M.M., Osman, S.A., Husam, O.A., et al. "Numerical study of the cyclic behavior of steel plate shear wall systems (SPSWs) with differently shaped openings", *Steel and Composite Structures*, **26**(3), pp. 361–373 (2018).
7. Barua, K. and Bhowmick, A.K. "Nonlinear seismic performance of code designed perforated steel plate shear walls", *Steel and Composite Structures*, **31**(1), pp. 85–98 (2019).
8. Guo, L., Rong, Q., Ma, X., et al. "Behavior of steel plate shear wall connected to frame beams only", *International Journal of Steel Structures*, **11**(4), pp. 467–479 (2011).
9. Jahanpour, A., Jönsson, A., and Moharrami, H. "Seismic behavior of semi-supported steel shear walls", *Journal of Constructional Steel Research*, **74**, pp. 118–133 (2012).
10. Bruneau, M., Uang, C.M., and Sabelli, R., *Ductile Design of Steel Structures*, McGraw Hill Professional, New York, NY, USA (2011).
11. Caccese, V., Elgaaly, M., and Chen, R. "Experimental study of thin steel-plate shear walls under cyclic load", *Journal of Structural Engineering*, **119**(2), pp. 573–587 (1993).
12. Sabouri-Ghomi, S. and Sajjadi, S.R.A. "Experimental and theoretical studies of steel shear walls with and without stiffeners", *Journal of Constructional Steel Research*, **75**, pp. 152–159 (2012).
13. Jin, S., Ou, J., and Liew, J.R. "Stability of buckling-restrained steel plate Shear walls with inclined-slots", Theoretical Analysis and Design Recommendations, J Constr Steel Res, **117**, pp. 13–23 (2016).
14. Valizadeh, H., Veladi, H., Farahm, B., et al. "Experimental investigation on cyclic behavior of butterfly-shaped link steel plate shear walls (BLSPSWs)", *Int. J. Eng., IJE Trans. B: Appl.*, **32**(11). pp. 1559–1569 (2019).
15. Formisano, A., Castaldo, C., and Chiumiento, G. "Optimal seismic upgrading of a reinforced concrete school building with metal-based devices using an efficient multi-criteria decision-making method", *Structure and Infrastructure Engineering*, **13**(11), pp. 1373–1389 (2017).
16. Shekastehband, B., Azaraxsh, A.A., and Showkati, H. "Hysteretic behavior of perforated steel plate shear walls with beam-only connected infill plates", *Steel and Composite Structures*, **25**(4), pp. 505–521 (2017).
17. Liu, W.Y., Li, G.Q., and Jiang, J. "Capacity design of boundary elements of beam-connected buckling restrained steel plate shear wall", *Steel and Composite Structures*, **29**(2), pp. 231–242 (2018).
18. Choi, I.R. and Park, H.G. "Steel plate shear walls with various infill plate designs", *Journal of Structural Engineering*, **135**(7), pp. 785–796 (2009).
19. Jahanpour, A., Moharrami, H., and Aghakoochak, A. "Evaluation of ultimate capacity of semi-supported steel shear walls", *Journal of Constructional Steel Research*, **67**(6), pp. 1022–1030 (2011).
20. Xu, T., Shao, J.H., Zhang, J.Y., et al. "Experimental performance evaluation of multi-storey steel plate shear walls designed by different methods", *International Journal of Civil Engineering*, **17**(7), pp. 1145–1154 (2019).
21. Qin, Y., Lu, J., and Cao, S. "Flexural behavior of beams in steel plate shear walls", *Steel and Composite Structures*, **23**(4), pp. 473–481 (2017).
22. Moghaddam, S.H. and Masoodi, A.R. "Elastoplastic nonlinear behavior of planar steel gabled frame", *Advances in Computational Design*, **4**(4), pp. 397–413 (2019).
23. Wei, M.W., Richard Liew, J.Y., and Fu, X.Y. "Nonlinear finite element modeling of novel partially connected buckling-restrained steel plate shear walls", *International Journal of Steel Structures*, **19**(1), pp. 28–43 (2019).
24. Abedini, M., Raman, S.N., Mutalib, A.A., et al. "Strengthening of the panel zone in steel moment-resisting frames", *Advances in Computational Design* (2019).
25. Jalali, S.A. and Darvishan, E. "Seismic demand assessment of self-centering steel plate shear walls", *Journal of Constructional Steel Research*, **162**, 105738 (2019).
26. Soltani, N., Karim Abedi, M.P., and Golabi, H. "An investigation of seismic parameters of low yield strength steel plate shear walls", *Earthquakes and Structures*, **12**(6), pp. 713–723 (2017).

27. Valizadeh, H., Farahmand Azar, B., Veladi, H., et al. "The shear capacity assessment of steel plate shear walls with peripheral circular holes", *Thin-Walled Structures*, **163**, 107638 (2021).

28. De Matteis, G., Formisano, A., Mazzolani, F.M., et al. "Design of low-yield metal shear panels for energy dissipation", *Improvement of Buildings' Structural Quality by New Technologies - Proceedings of the Final Conference of COST Action C12*, pp. 665–675 (2005).

29. Formisano, A., Mazzolani, F.M., Brando, G., et al. "Numerical evaluation of the hysteretic performance of pure aluminium shear panels", *Proceedings of the 5th International Conference on Behaviour of Steel Structures in Seismic Areas - Stessa 2006*, pp. 211–217 (2006).

30. Formisano, A., Mazzolani, F.M., and De Matteis, G. "Numerical analysis of slender steel shear panels for assessing design formulas", *International Journal of Structural Stability and Dynamics*, **7**(2), pp. 273–294 (2007).

31. ASCE/SEI 7-16 "Minimum design loads and associated criteria for buildings and other structures", *American Society of Civil Engineers*, Reston, VA, Fairfax (2017).

32. Amani, M., Alinia, M.M., and Fadakar, M. "Mperfection sensitivity of slender/stocky metal plates", *Thin-Walled Structures*, **73**, pp. 207–215 (2013).

33. Jahanpour, A. and Moharrami, H. "Evaluation of behavior of the secondary columns in semi-supported steel shear walls", *Thin-Walled Structures*, **93**, pp. 94–101 (2015).

34. Broujerdian, V., Shayanfar, M., and Ghamari, A. "Corner crack effect on the seismic behavior of steel plate shear wall system", *Civil Engineering Infrastructures Journal*, **50**(2), pp. 311–332 (2017).

35. Ghadami, A., Pourmoosavi, G., and Ghamari, A. "Seismic design of elements outside of the short low-yield-point steel shear links", *Journal of Constructional Steel Research*, **178**, 106489 (2021).

36. Broujerdian, V., Ghamari, A., and Ghadami, A. "An investigation into crack and its growth on the seismic behavior of steel shear walls", *Thin-Walled Structures*, **101**, pp. 205–212 (2016).

37. Alavi, E. and Nateghi, F. "Experimental study on diagonally stiffened steel plate shear walls with central perforation", *Journal of Constructional Steel Research*, **89**, pp. 9–20 (2013).

38. Hosseinzadeh, S.A.A. and Tehranizadeh, M. "Introduction of stiffened large rectangular openings in steel plate shear walls", *Journal of Constructional Steel Research*, **77**, pp. 180–192 (2012).

Biographies

Vahid Broujerdian is an Assistant Professor of Structural Engineering and the Head of Structural Enginnering Group at the School of Civil Engineering at Iran University of Sciecne and Technology. He received his BSc (2002), MSc (2004), and PhD (2010) in Structural Engineering from Sharif University of Technology, Tehran, Iran. His research interests include analytical and numerical study of the nonlinear behavior of materials and structures, design and analysis of wind and earthquake-resistsnt structures, and design and analysis of structures against abnormal conditions (impact, blast, and fire).

Ramin Pahnabi is highly motivated and has recently graduated from one of the top four universities in Iran with the degree of Master of Science in Civil Engineering (structural Engineering). He was employed by Pardisan Sazeh Consulting Engineers Company as a structural expert, a company with reputation for Engineering Excellence and Technical Innovation since July 2019. He holds two scholarships for BSc and MSc courses, the latter achieved by ranking 250 out of 50000 applicants. He is a competent IT user, having substantial skills in simulation using software's packages such as ABAQUS.

Ali Ghamari is Assistant Professor at Islamic Azad Uiversity, Ilam, Iran and a visiting Assistant Professor at Arya University of Scince and Sustainability, Tehran, Iran. He has been the Head of Futurology Reasech Center in Scince and Technolgy, IAU, Iran since 2019. He recived PhD (2017) in Structural Engineering from Iran University of Sciecne and Technology. He completed reseach program of PostDoc postion at Sharif University of Sceince and Technology in 2019 on introducing an innovative infill wall made of lihtweigh concrete and fibers. His research interests include seismic behabior of structures, dampers, and fiber-reinforced concrete.